JOURNAL OF GEOPHYSICAL RESEARCH, VOL. 98, NO. C11, PAGES 20,299–20,305, NOVEMBER 15, 1993

Observations of Nonlinear Interactions in Directionally Spread Shoaling Surface Gravity Waves

STEVE ELGAR

School of Electrical Engineering and Computer Science, Washington State University, Pullman

R. T. GUZA

Center for Coastal Studies, Scripps Institution of Oceanography, La Jolla, California

M. H. FREILICH

College of Oceanography, Oregon State University, Corvallis

Shoaling wave fields generated in laboratory experiments were analyzed to determine the sensitivity of nonlinear interactions to the directional distributions of incident waves. Peaks in the directional spectra observed in shallow water were consistent with near-resonant, quadratic interactions between two primary waves transferring energy to a third wave with the sum frequency and vector sum wavenumber of the primary waves. Directionally colinear waves forced a higher-frequency wave propagating in the same direction as the primary waves, while directionally spread (i.e., noncolinear) primary waves forced a higher-frequency wave that propagated in a direction between those of the interacting primary waves. Deepwater wave fields with similar frequency spectra but different directional spectra evolved to different shallow-water directional spectra, yet their shallow-water frequency spectra were remarkably similar. This result suggests that the shape of the directional spectrum of the incident wave field has only a small effect on the magnitudes of nonlinear energy transfers during shoaling. The principal effect of directionality in the incident wave field is on the directions, not the amplitudes, of the nonlinearly generated waves. The laboratory data demonstrate clearly the importance of triad interactions between noncolinear and colinear shoaling waves.

1. INTRODUCTION

Ocean surface gravity waves evolve significantly as they propagate shoreward into shoaling water. Although linear theory predicts the observed increasing wave amplitudes and narrowing directional distributions of swell and sea waves, nonlinear effects are important.

Well seaward of the shoaling region ($|\mathbf{k}|h > 0(1)$, where $\mathbf{k}$ is a typical wavenumber and h is the water depth), the wave field is characterized by strong frequency dispersion and broad directional distributions. At second order in weakly nonlinear theory, forced motions arise which can be interpreted as small corrections to the underlying linear wave field. Resonances between quartets of waves occur at the next higher order, resulting in slow cross-spectral energy transfers. Although energy exchanges are very small on wavelength scales, the frequency-directional spectrum is substantially modified over hundreds of wavelengths [*Phillips*, 1960; *Hasselmann*, 1962, and others].

In very shallow water ($|\mathbf{k}|h \ll 1$; within the surf zone, for example), waves are essentially nondispersive, directional distributions are narrow, and strong nonlinearities drive relatively rapid spectral evolution. Models based on the nondispersive, nonlinear shallow-water equations for unidirectional waves [*Hibberd and Peregrine*, 1979] predict many important features of bore propagation and run-up [*Kobayashi et al.*, 1989, and references therein].

Paper number 93JC02213.
0148-0227/93/93JC-02213$05.00

Between the strongly dispersive deepwater and nondispersive surf zone regimes is the shoaling region, characterized by moderate dispersion, narrow (but measurable) directional spread, and substantial nonlinearity. Waves propagating through the shoaling region evolve significantly in several (rather than hundreds of) wavelengths, with nonlinearly driven cross-spectral transfers of energy and phase modifications leading to the asymmetric and skewed profiles characteristic of nearly breaking and broken waves [*Freilich and Guza*, 1984; *Elgar and Guza*, 1985, 1986; *Elgar et al.*, 1990*b*]. The present work concerns the evolution of the frequency-directional spectra of shoaling waves.

The short evolution distances and moderate dispersion characteristic of the shoaling region suggest that second-order (quadratic) nonlinearities involving wave triads are important [*Armstrong et al.*, 1962; *Bretherton*, 1964]. Nonlinear triad interactions occur among waves with frequencies and wavenumbers such that

$$f_1 + f_2 - f_3 = 0 \tag{1a}$$

$$\mathbf{k}_1 + \mathbf{k}_2 - \mathbf{k}_3 = 0, \tag{1b}$$

where f_i and $\mathbf{k}_i$ are the scalar frequency and vector wavenumber, respectively, of the ith wave. For weakly nonlinear quadratic sum interactions, the wave components 1 and 2 each obey the lowest-order (linear) dispersion relation

$$|\mathbf{k}| = L(f). \tag{1c}$$

The physical interpretation of (1*a*) and (1*b*) is that the sum interaction between wave components 1 and 2 forces mo-

tions with the scalar sum frequency and the vector sum wavenumber. This is true both when component 3 does not obey (1*c*) (the "bound corrections" of dispersive waves [*Hasselmann*, 1962]) and when the sum component exactly satisfies the dispersion relation (1*c*) ("resonant" interactions [*Armstrong et al.*, 1962]). In the nonresonant case, energy transfers are small, whereas in the resonant case, energy transfers between all three modes can be large.

Armstrong et al. [1962] showed that significant energy also can be exchanged between the three waves of the triad if the sum component nearly satisfies the dispersion relation ("near-resonant" interactions). Defining $|\mathbf{k}_\delta|$ as the difference between the free ($|\mathbf{k}_3| = L(f_3)$) and the sum ($|\mathbf{k}_1 + \mathbf{k}_2|$) wavenumber magnitudes

$$|\mathbf{k}_\delta| = |\mathbf{k}_1 + \mathbf{k}_2| - |\mathbf{k}_3|, \tag{2a}$$

the normalized wavenumber magnitude mismatch

$$\delta = |\mathbf{k}_\delta|/|\mathbf{k}_3| \tag{2b}$$

is a measure of the departure from exact resonance [*Freilich and Guza*, 1984]. When the mismatch is small, phase relationships (and thus the magnitudes and signs of energy transfers) between the interacting waves vary only slightly over a wavelength, allowing significant integrated cross-spectral energy transfer over several wavelengths.

The mismatch δ can arise from dispersion in a triad involving colinear primary waves, from directional differences in a triad involving nondispersive waves, or from both dispersion and directional differences in the triad components. In shallow water, δ is $O(kh)^2$. For wave components obliquely incident on a beach with plane parallel contours (refracting according to Snell's law), straightforward algebra demonstrates that

$$\lim_{|\mathbf{k}h|\to 0} \delta \propto \frac{|\mathbf{k}_1|\,|\mathbf{k}_2|}{|\mathbf{k}_3|^2}\,[(|\mathbf{k}_1| + |\mathbf{k}_2|)h]^2 \cdot \left\{1 + \frac{(|\mathbf{k}_1|\,\sin\theta_{1,0} - |\mathbf{k}_2|\,\sin\theta_{2,0})^2}{(|\mathbf{k}_1| + |\mathbf{k}_2|)^2}\right\} + O[(kh)^4], \tag{3}$$

where $\theta_{1,0}$ and $\theta_{2,0}$ are the deepwater propagation directions of wave components 1 and 2. The normalized mismatch δ in shallow water is thus not very sensitive to deepwater directional differences between the interacting waves, varying by at most a factor of 2 (and then only for the extreme case of primary waves arriving from opposite quadrants at grazing incidence [*Herbers et al.*, 1993]). Equation (3) formally demonstrates that the wavenumber mismatch resulting from directional spreading is never larger than the mismatch owing to frequency dispersion if the primary waves have impinged on the beach from deep water and refracted approximately according to Snell's law. *Freilich et al.* [1990] (hereafter referred to as FGE) illustrated this general result (see their Figure 7) with a specific case example.

Deterministic models incorporating near-resonant triad interactions based on the weakly nonlinear, weakly dispersive Boussinesq equations [*Peregrine*, 1967, 1972] have been developed for a one-dimensional plane wave [*Mei and Ünlüata*, 1972], a spectrum of normally incident waves on a plane beach [*Freilich and Guza*, 1984], and two-dimensional wave fields [*Liu et al.*, 1985]. The near-resonant formalism of Boussinesq shoaling models allows interactions between waves not exactly satisfying (1*b*), and weakly dispersive waves with some directional spread can be accommodated. In deterministic shoaling models based on the Boussinesq equations, energy transfers over relatively short evolution distances are driven by near-resonant interactions involving both colinear and noncolinear waves. Frequency dispersion is at least as important as directional spreading (e.g., equation (3) and *Freilich and Guza*, 1984).

Predictions of a one-dimensional, near-resonant Boussinesq model have been successfully compared to both a plane wave in the laboratory [*Mei and Ünlüata*, 1972] and field observations. The waves in the field observations had small directional spread and a range of initial (e.g., at the seaward edge of the shoaling region) frequency spectra [*Freilich and Guza*, 1984; *Elgar and Guza*, 1985, 1986; *Elgar et al.*, 1990*a*, and references therein]. The model calculations neglected the mismatch resulting from the directionally spread waves, but the model still accurately predicted transformations of quantities such as frequency spectra and bispectra (all based on the complex Fourier coefficients of the wave field). Two-dimensional extensions of the model have been compared successfully to laboratory observations of nonrandom shoaling waves [*Liu et al.*, 1985].

Although there are many observations of the evolution of the frequency spectra of shoaling waves, observations of the directional properties are quite limited. FGE presented a single case study on a near-planar natural beach. *Elgar et al.* [1992] showed that appropriately scaled directional wave fields in the laboratory evolved in a manner qualitatively similar to those measured by FGE in the field. In both the field and the laboratory, the frequency-directional spectrum measured in shallow water deviated significantly from the predictions of two-dimensional linear theory [*Collins*, 1972; *Le Méhauté and Wang*, 1982].

Recently, *Abreu et al.* [1992] (hereafter referred to as ALT) developed a statistical model for the nonlinear evolution of the frequency-directional spectrum. The model is based on the nondispersive, nonlinear shallow-water ($\mathbf{k}h \ll 1$) equations and a natural asymptotic closure [*Newell and Aucoin*, 1971] for directionally spread, nondispersive waves. A consequence of the statistical model formulation (and the asymptotic closure) is that nonlinear spectral evolution results only from exactly resonant interactions ($|\mathbf{k}_\delta| = 0$). Since the waves are assumed frequency nondispersive in the ALT formalism, only triads containing waves traveling in the same direction (i.e., with colinear wavenumber vectors, equation (1*b*)) are considered resonant.

Armstrong et al. [1962] pointed out that mismatches can eventually change the sign of energy transfers, and thus the asymptotic effect of near-resonances may be small. Note, however, that high-order terms in the full equations (neglected in the approximate Boussinesq and nondispersive shallow-water models) may be important at large distances, and asymptotic results from these approximate models may not be valid [*Freilich and Guza*, 1984; *Elgar et al.*, 1990*a*]. In any event, asymptotic solutions are not relevant to the wave fields considered here (and on many natural beaches) because modifications to the shoaling waves occur on scales $O(5–10)$ wavelengths.

When applying their model to shoaling waves, ALT neglect the mismatch owing to frequency dispersion because it "represents a small departure from the strict applicability of the model and is a compromise between the classical shallow

TABLE 1. Parameters for the Four Laboratory Data Sets

Data Set	Δf, Hz	H_{sig}, cm			Dissipation, %
		Deep	Shallow	lfdt	
S10	0.049	3.4	3.8	4.0	5
GBM81	0.059	8.2	8.1	8.9	9
GBM85	0.059	7.9	7.7	8.6	10
GBM71	0.059	7.6	7.8	8.8	11

The frequency resolution is given by Δf. Multiply the dimensionless band number in the power, directional, and bicoherence spectra (Figures 1–6) by Δf to convert to the dimensional frequency. The H_{sig} columns are the significant wave heights observed in deep and shallow water and predicted in shallow water (linear finite-depth therory (lfdt)) using the deepwater directional spectrum and linear finite-depth theory [*Le Méhauté and Wang*, 1982]. A rough measure of the amount of breaking-induced dissipation is given in the last column on the right, which is the percent reduction in observed shallow-water wave height relative to that predicted by linear finite-depth theory.

water criterion and the range of strong interactions" suggested by the results of FGE and *Elgar et al.* [1992]. ALT thus implicitly assume that colinear interactions are closer to resonance (smaller δ) and are therefore more important than the neglected noncolinear interactions. However, as demonstrated by (3) and FGE's Figure 7, deviations from exact resonance owing to directional spreading are typically smaller than deviations owing to frequency dispersion.

ALT simulated the FGE data, and their nondispersive statistical model predicted well the observed evolution of the frequency-directional spectrum. They therefore concluded that overlaps in directional spectra of the primary waves provided sufficient colinear energy to drive significant resonant energy transfers to the sum frequency.

FGE suggested that the observed evolution of the shoaling, two-dimensional wave field was consistent with near-resonant (including both colinear and noncolinear) triad interactions. ALT argued that the success of the nondispersive statistical model demonstrated that purely resonant interactions between colinear waves were responsible for the observed spectral evolution and that the noncolinear interactions of the discrete Boussinesq models were actually unimportant.

Owing to the relatively large overlaps between directional spectra at different frequencies, the data presented by FGE are insufficient to determine whether colinear interactions alone (ALT) or both colinear and noncolinear interactions (FGE) are responsible for the observed evolution at the sum frequencies of the component waves. In the present study, the shoaling evolution of laboratory wave fields with directional spectra designed to eliminate overlap between interacting waves is investigated. The laboratory observations are presented and discussed in terms of potential interactions between colinear and noncolinear waves in section 2. Results are summarized in section 3.

2. LABORATORY OBSERVATIONS

2.1. *Laboratory Experiments and Data Reduction*

The laboratory basin, located at the U.S. Army Engineer Waterways Experiment Station's Coastal Engineering Research Center, has been described in detail by *Vincent and Briggs* [1989], *Elgar et al.* [1992], and researchers referred to therein. For the present study, the basin dimensions were approximately 40 m alongshore by 28 m cross-shore, with a 0.033 slope beach extending about 15 m seaward from the still-water shoreline to a constant depth portion of the basin. The wave generator was 4.5 m seaward of the toe of the sloping concrete beach in a constant depth of 50 cm.

Capacitance-type wave elevation sensors [*Briggs and Hampton*, 1987] were sampled at 10 Hz for 512 s for most data sets (Table 1). Statistics presented in the following sections are averages over 10 short records of 51.2-s duration and three neighboring frequency bands, with a frequency resolution of 0.059 Hz and 60 degrees of freedom. (The S10 data were processed slightly differently and have 250 degrees of freedom and a frequency resolution of 0.049 Hz. See *Elgar et al.* [1992] for details.)

An alongshore-oriented array of wave staffs (the "deep array") was located 7.5 m shoreward of the wave generator, 3 m up the slope, in a depth of 40 cm. A similar array was located in shallow water (16-cm depth). Both arrays had an 8-1-3-2-5 lag configuration, with unit lags of 85 and 55 cm in deep and shallow water, respectively. Directional spectra were estimated using an iterated maximum likelihood method [*Pawka*, 1983; FGE].

2.2. *Previous Experiments*

At the laboratory deep array, the S10 directional wave field (see Table 1 for dimensional parameters) replicated the wave field measured at the deep field array reported by FGE. The evolution of the laboratory and ocean wave fields was also nearly identical (with suitable normalization), confirming that the laboratory simulations are accurate proxies for field observations, at least for these wave and beach conditions [*Elgar et al.*, 1992].

The observed shallow-water S10 frequency (i.e., nondirectional) spectrum (Figure 1) was elevated at bands 16 ($2f_1$) and 23 ($3f_1$) (e.g., harmonics of the dominant "swell" in band 8 (f_1)) relative to predictions using linear theory (initialized with the measured deepwater frequency-directional spectrum shown in Figure 2*a*). The observed frequency-directional spectrum in shallow water (Figure 2*c*) was also different from that predicted by linear theory (Figure 2*b*). In particular, linear theory did not predict the peaks in bands 16 and 23 approximately aligned with the local direction of the swell (band 8) or the peak at band 21 ($f_1 + f_2$) intermediate in direction between the directional peaks of the swell (band 8, f_1) and the higher-frequency "sea" (band 13, f_2) (Figures 2*d* and 2*f*). (For convenience, the lower- and higher-frequency peaks in the bimodal fre-

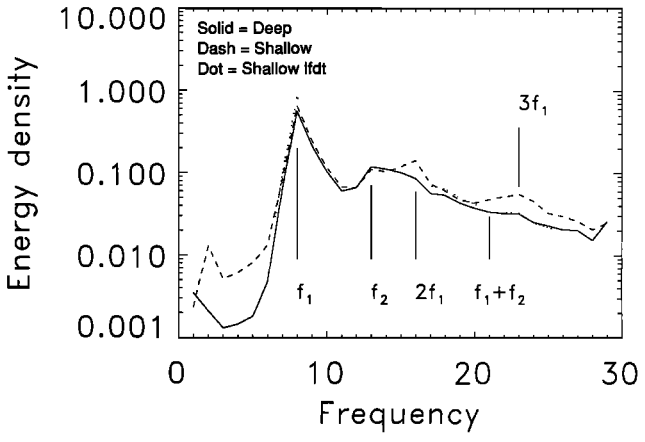

Fig. 1. Energy density (arbitrary units) versus frequency (units are band numbers; see Table 1 for dimensional values) for the S10 wave field. The solid curve is the observed deepwater spectrum, the dashed curve is the observed shallow-water spectrum, and the dotted curve is the shallow-water spectrum predicted by linear finite-depth theory (lfdt) given the deepwater directional spectrum.

quency spectra discussed here will be referred to as swell and sea peaks, respectively.)

2.3. *New Laboratory Experiments*

In the S10 wave field, the swell (f_1) had much more energy than the sea (f_2) (Figure 1), and there was considerable directional overlap between the swell and the sea (Figure 2*d*). Three additional wave fields, more strongly bimodal in both frequency and direction, were generated. All of these wave fields had approximately equal swell and sea energies in deep water, and two had little directional overlap between the deepwater swell and sea.

The first experiment compared the evolution of two deepwater wave fields (GBM81 and GBM85; Table 1) that had nearly identical frequency spectra but different directional distributions. The deepwater frequency spectra were dominated by (nearly equal) energy at frequency bands 7 (swell, f_1) and 14 (sea, f_2) (Figure 3*a*). GBM81 was directionally unimodal, with all waves normally incident (not shown). GBM85 was directionally bimodal, with ~19° difference in the deepwater propagation direction of the normally incident swell (f_1) and the obliquely incident sea (f_2) (Figures 3*b* and 3*d*) and little directional overlap at either the deep or the shallow array (Figures 3*d* and 3*e*). The largest directional overlap between f_1 and f_2 in GBM85 was actually at normal incidence (~0°), where frequency f_2 has a secondary directional peak (Figure 3*d*).

If only colinear interactions transfer significant energy, it would be expected that the energy in band 21 ($f_1 + f_2$) in GBM81 (where all the primary wave energy was essentially colinear) would be larger than that in GBM85 (where much of the primary wave energy propagated with significantly different directions). However, despite the differences in the deepwater directional spectra, GBM81 and GBM85 had nearly identical shallow-water frequency spectra (Figure 3*a*), with nonlinearly generated peaks at bands 21 ($3f_1 = f_1 + f_2$) and 28 ($2f_2$), the harmonics and/or combination tones of the swell and sea in deep water.

The observed elevated energy at band 21 in the directionally bimodal GBM85 (Figure 3*a*) could have resulted from the combination interaction between the swell and the sea

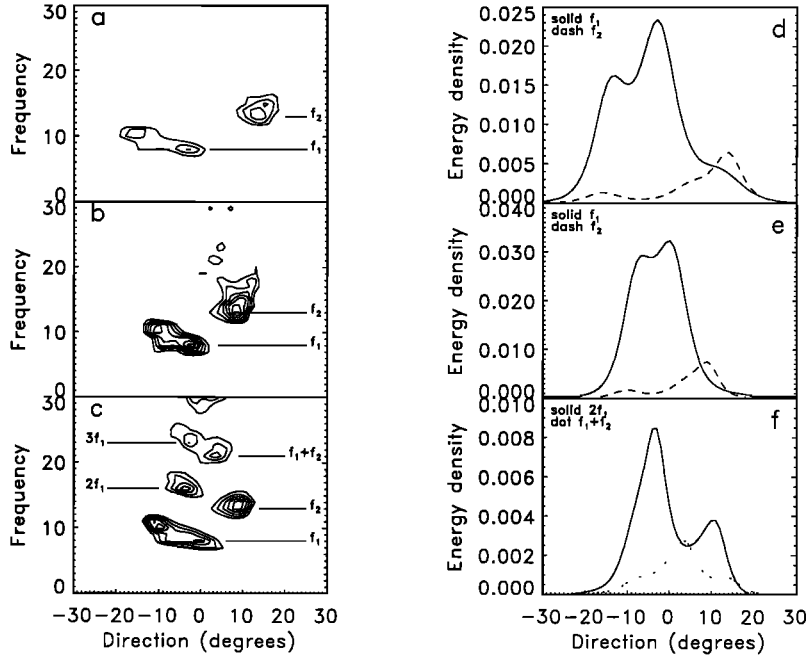

Fig. 2. Frequency-directional spectra for the S10 wave field (*a*) observed in deep water, (*b*) predicted by linear finite-depth theory in shallow water, and (*c*) observed in shallow water. At each frequency the variance is distributed linearly with direction, and the area under the curve at each frequency is proportional to the logarithm of the spectral density at that frequency. (In other words, the plot is linear in direction but log in frequency.) (*d*) Observed deepwater energy density versus direction for band 8 (f_1; solid curve) and band 13 (f_2; dashed curve); (*e*) observed shallow-water energy density versus direction for band 8 (f_1; solid curve) and band 13 (f_2; dashed curve); (*f*) observed shallow-water energy density versus direction for band 16 ($2f_1$; solid curve) and band 21 ($f_1 + f_2$; dotted curve).

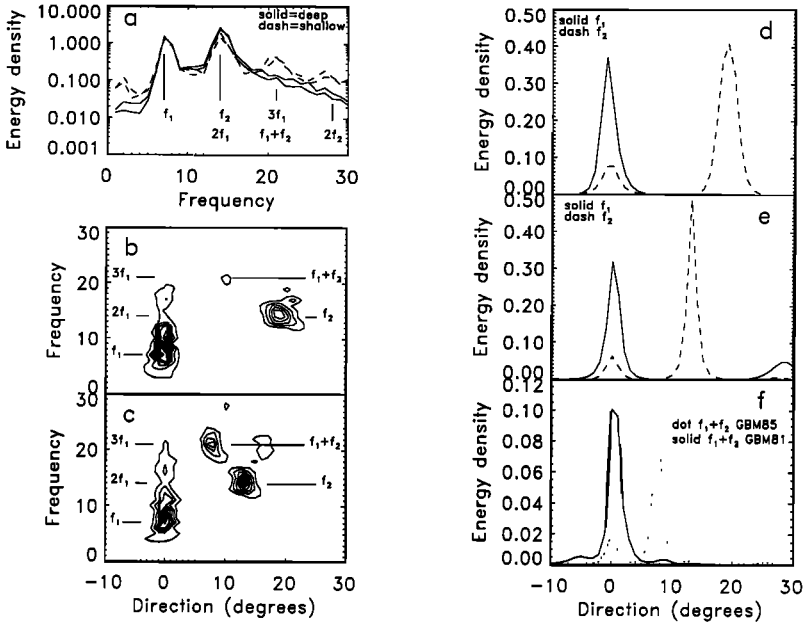

Fig. 3. (*a*) Energy density versus frequency for the wave fields GBM81 and GBM85 (no attempt has been made to distinguish between them). The solid curves are the observed deepwater spectra, and the dashed curves are the observed shallow-water spectra. (*b*) GBM85 frequency-directional spectrum observed in deep water; (*c*) GBM85 frequency-directional spectrum observed in shallow water; (*d*) GBM85 observed deepwater energy density versus direction for band 7 (f_1; solid curve) and band 14 (f_2; dashed curve); (*e*) GBM85 observed shallow-water energy density versus direction for band 7 (f_1; solid curve) and band 14 (f_2; dashed curve); (*f*) observed shallow-water energy density versus direction for band 21 ($f_1 + f_2$) for GBM85 (noncolinear waves; dotted curve) and GBM81 (colinear waves; solid curve).

($f_1 + f_2$) or (more improbably) from a higher-order quartet interaction forcing the third harmonic of the swell ($3f_1$) directly. Band 7 was normally incident, and the maximum directional overlap between bands 7 (f_1) and 14 (f_2) was also at 0° (Figures 3*d* and 3*e*). Thus the two possible colinear interactions at band 21 both had maximum forcing at 0°. Although a secondary peak in band 21 was observed at 0° in shallow water, the maximum occurred at 8° (Figure 3*f*), nearly the direction (9°) of the vector sum of the band 7 and 14 wavenumbers.

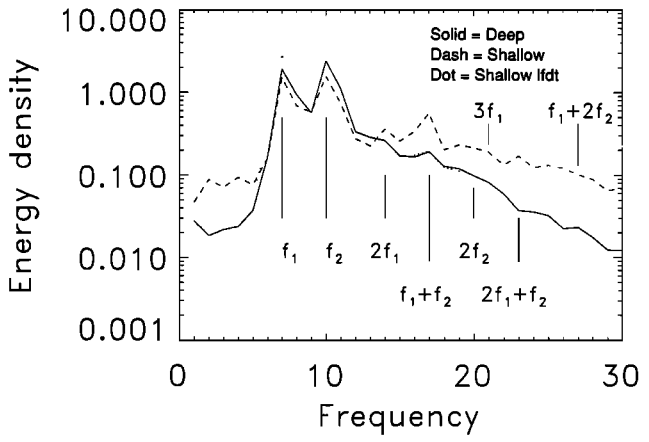

Fig. 4. Energy density versus frequency for the GBM71 wave field. The solid curve is the observed deepwater spectrum, the dashed curve is the observed shallow-water spectrum, and the dotted curve is the shallow-water spectrum predicted by linear finite-depth theory given the deepwater directional spectrum.

The additional secondary peak at 17° in band 21 (Figure 3*f*) was close to the vector sum direction (18°) of the band 7 secondary peak at 28° and the band 14 primary peak at 13° (Figure 3*e*). The deepwater waves at 28° in band 7 were generated inadvertently by the mechanical wave paddle but were free to interact as they shoaled. As shown in Figure 3*f*, despite their approach to the beach at a relatively high angle, these waves participated in a noncolinear, near-resonant triad interaction. Thus, of the three directional peaks in band 21, only the secondary peak at 0° was driven by colinear interactions.

The deepwater frequency spectrum of an additional new wave field (GBM71; Table 1 and Figure 4) was bimodal, with approximately equal power spectral levels $E(f)$ at bands 7 (f_1) and 10 (f_2), in contrast to S10, for which $E(f_1) \gg E(f_2)$ (Figure 1). Unlike GBM81 and GBM85, f_1 and f_2 for S10 and GBM71 were not integral multiples of each other. The 20° separation between the peak directions of these bands in GBM71 was similar to that for S10, but the deepwater directional spread at each of the energy-containing frequencies was much less than that for S10 (compare Figures 2*a* and 2*d* with 5*a* and 5*d*). At frequencies above those corresponding to the primary waves (f_1 and f_2), the levels of the GBM71 frequency spectrum observed in shallow water were greater than those predicted by linear theory. Peaks were discernible at bands 14 (corresponding to $2f_1$), 17 ($f_1 + f_2$), 20 ($2f_2$), and 23 ($2f_1 + f_2$) (Figure 4). The observed shallow-water directions of the primary waves (frequencies f_1 and f_2; Figure 5*c*) approximately corresponded to linearly refracted versions (Figure 5*b*) of their measured deepwater distributions (Figure 5*a*). The harmonic peaks at $2f_2$, $2f_1$, and $3f_1$ were approximately aligned

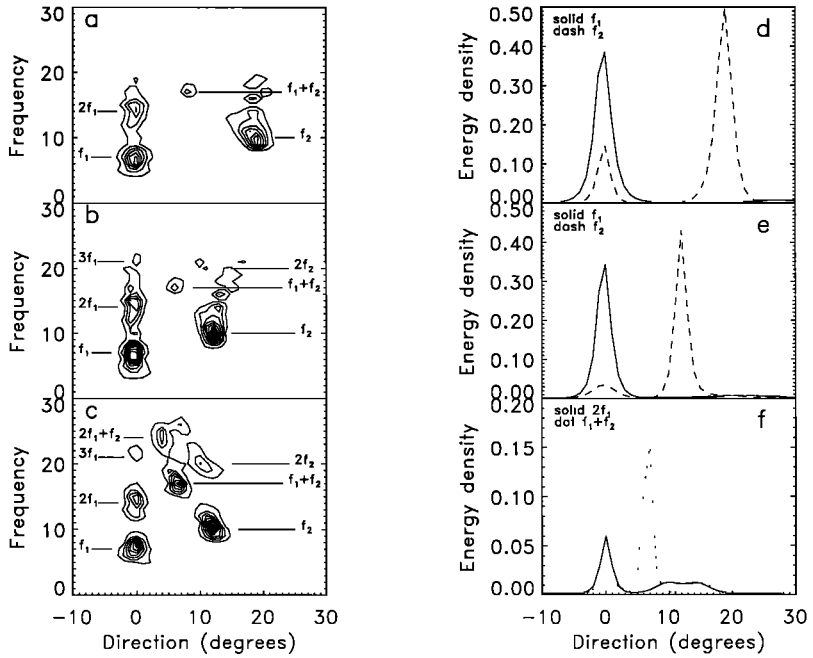

Fig. 5. Frequency-directional spectra for the GBM71 wave field (*a*) observed in deep water, (*b*) predicted by linear finite-depth theory for shallow water, and (*c*) observed in shallow water; (*d*) observed deepwater energy density versus direction for band 7 (f_1; solid curve) and band 10 (f_2; dashed curve); (*e*) observed shallow-water energy density versus direction for band 7 (f_1; solid curve) and band 10 (f_2; dashed curve); (*f*) observed shallow-water energy density versus direction for band 14 ($2f_1$; solid curve) and band 17 ($f_1 + f_2$; dotted curve).

with the directions of the respective primary peaks at f_1 and f_2.

The directions of peaks at the combination frequencies ($f_1 + f_2$ and $2f_1 + f_2$) were between the swell and sea directions (Figure 5*c*). The directional overlap between bands 7 (f_1) and 10 (f_2) was small and occurred at 0° in both deep and shallow water (Figures 5*d* and 5*e*). If colinear interactions were more important than noncolinear interactions, the band 17 ($f_1 + f_2$) directional spectrum would be expected to be largest at 0°. As shown in Figure 5*f*, the energy at 0° was relatively low, and most of the energy in band 17 was centered at 7° (the direction of the vector sum of the peak wavenumbers of bands 7 and 10 in shallow water). The direction of the band 24 peak ($2f_1 + f_2$; Figure 5*c*) corresponds to the direction of the vector sum of the shallow-water peak wavenumbers of bands 7 (f_1) and 17 ($f_1 + f_2$).

The nonlinear origins of all harmonic and combination spectral peaks of the GBM71 wave field were confirmed by bicoherence spectra (Figure 6). The shallow-water bicoherence was comparably strong for harmonic interactions (between colinear waves denoted by A, B, and F in Figure 6*b*) and combination interactions (between noncolinear waves denoted by C, D, E, and G in Figure 6*b*). Phase coupling involving the combination tones could be detected both in deep (Figure 6*a*) and shallow (Figure 6*b*) water, where the angular separation of the swell and sea directional peaks was approximately 20° and 8°, respectively.

The shallow directional spectra for S10, GBM85, and GBM71 (Figures 2*c*, 3*c*, and 5*c*, respectively) were consistent with the importance of both colinear and noncolinear triad interactions, as were the bicoherence spectra (Figure 6 for GBM71; Figure 7 in *Elgar et al.* [1992] for S10). In all cases, harmonic waves were directionally aligned with the

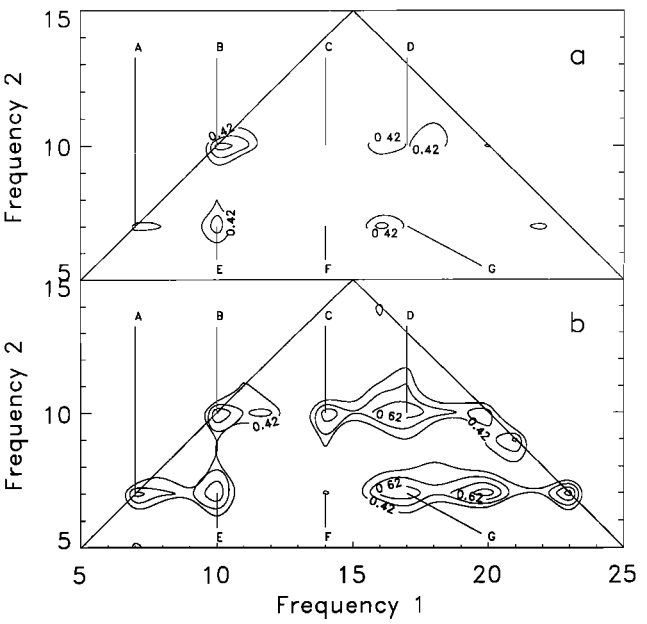

Fig. 6. Contours of bicoherence for the GBM71 wave field shown in Figures 4 and 5. (*a*) Water depth is 35 cm; (*b*) water depth is 16 cm. Contours indicate statistically significant nonlinear interactions between triads of waves with frequencies given by frequency 1, frequency 2, and frequency 3 (= frequency 1 + frequency 2). The alphabetically labeled vertical lines terminate at (frequency 1, frequency 2) coordinates corresponding to the following wave triads: A, $f_1, f_1, 2f_1$; B, $f_2, f_2, 2f_2$; C, $2f_1, f_2, 2f_1 + f_2$; D, $f_1 + f_2, f_2, f_1 + 2f_2$; E, $f_2, f_1, f_1 + f_2$; F, $2f_1, f_1, 3f_1$; G, $f_1 + f_2, f_1, 2f_1 + f_2$, where f_1 = band 7 and f_2 = band 10. The minimum contour plotted (0.42) is statistically significant, and additional contours are plotted every 0.1. Interactions involving infragravity waves (band numbers less than 5) are not shown, and the contours extending slightly outside the triangle are plotting artifacts.

primary waves (e.g., $2f_1$ is aligned with f_1, a colinear interaction). The wavenumbers of waves at combination frequencies (e.g., $f_1 + f_2$) corresponded to the vector sum of the wavenumbers of the component primary waves (e.g., f_1 and f_2), consistent with (1*b*). Although the source (i.e., colinear or noncolinear) of energy at $f_1 + f_2$ is ambiguous in S10, it is clearly a noncolinear interaction in GBM71 and GBM85.

3. Conclusions

The frequency-directional spectra of shoaled waves observed in the field and laboratory are significantly different from those predicted by linear theory. For the laboratory data presented here, when the offshore frequency spectrum was bimodal with peaks at swell and sea frequencies, the observed shallow-water spectrum had additional peaks at frequencies corresponding to harmonics and combination tones of the deepwater swell and sea. The harmonics propagated in the same direction as the corresponding primary wave. However, waves with frequencies corresponding to the combination tones (e.g., frequencies equal to the sum of the swell and sea frequencies) propagated in directions very close to the direction of the vector sum of the swell and sea wavenumbers. The amount of energy transferred to the combination tones was observed to be a weak function of the angular separation between the swell and the sea. Moderate directional differences between the interacting waves had little effect on the evolution of the frequency spectrum, and thus the power spectrum observed in shallow water was unaltered when a directionally spread wave field was replaced with a nearly identical but colinear wave field. These laboratory observations are consistent with the physics of near-resonant, nonlinear triad interactions involving both colinear and noncolinear waves.

Acknowledgments. Support for this analysis was provided by the Physical Oceanography Program of the National Science Foundation, the Office of Naval Research (Coastal Sciences and Nonlinear Ocean Waves ARI), and the Modelling, Data, and Information Systems Branch of NASA. The generosity of J. Medina (Universidad Politécnica de Valencia) and support provided by the Dirección General de Investigación Científica y Técnica of Spain while the manuscript was being prepared are warmly and gratefully acknowledged, as is the assistance of M. Briggs, USACOE, in obtaining the laboratory data.

References

Abreu, M., A. Larraza, and E. Thornton, Nonlinear transformation of directional wave spectra in shallow water, *J. Geophys. Res.*, *97*, 15,579–15,589, 1992.

Armstrong, J. A., N. Bloembergen, J. Ducuing, and P. S. Pershan, Interactions between light waves in a nonlinear dielectric, *Phys. Rev.*, *127*, 1918–1939, 1962.

Bretherton, F. P., Resonant interactions between waves: The case of discrete oscillations, *J. Fluid Mech.*, *20*, 457–480, 1964.

Briggs, M. J., and M. L. Hampton, Directional spectral wave generator basin response to monochromatic waves, *Tech. Rep. CERC 87-6*, pp. 1–90, Coastal Eng. Res. Cent., U.S. Army Eng. Waterways Exp. Stn., Vicksburg, Miss., 1987.

Collins, J. I., Prediction of shallow-water spectra, *J. Geophys. Res.*, *77*, 2693–2707, 1972.

Elgar, S., and R. T. Guza, Shoaling gravity waves: Comparisons between field observations, linear theory, and a nonlinear model, *J. Fluid Mech.*, *158*, 47–70, 1985.

Elgar, S., and R. T. Guza, Nonlinear model predictions of bispectra of shoaling surface gravity waves, *J. Fluid Mech.*, *167*, 1–18, 1986.

Elgar, S., M. H. Freilich, and R. T. Guza, Recurrence in truncated Boussinesq models for nonlinear waves in shallow water, *J. Geophys. Res.*, *95*, 11,547–11,556, 1990*a*.

Elgar, S., M. H. Freilich, and R. T. Guza, Model-data comparisons of moments of nonbreaking shoaling surface gravity waves, *J. Geophys. Res.*, *95*, 16,055–16,063, 1990*b*.

Elgar, S., R. T. Guza, M. H. Freilich, and M. J. Briggs, Laboratory simulations of directionally spread shoaling waves, *J. Waterw. Port Coastal Ocean Div. Am. Soc. Civ. Eng.*, *118*, 87–103, 1992.

Freilich, M. H., and R. T. Guza, Nonlinear effects on shoaling surface gravity waves, *Philos. Trans. R. Soc. London, Ser. A*, *311*, 1–41, 1984.

Freilich, M. H., R. T. Guza, and S. Elgar, Observations of nonlinear effects in directional spectra of shoaling surface gravity waves, *J. Geophys. Res.*, *95*, 9645–9656, 1990.

Hasselmann, K., On the non-linear energy transfer in a gravity-wave spectrum, 1, General theory, *J. Fluid Mech.*, *12*, 481–500, 1962.

Herbers, T. H. C., R. L. Lowe, and R. T. Guza, Field observations of orbital velocities and pressure in weakly nonlinear surface gravity waves, *J. Fluid Mech.*, *245*, 413–435, 1993.

Hibberd, S., and D. H. Peregrine, Surf and runup on a beach: A uniform bore, *J. Fluid Mech.*, *95*, 323–345, 1979.

Kobayashi, N., G. DeSilva, and K. Watson, Wave transformation and swash oscillations on gentle and steep slopes, *J. Geophys. Res.*, *94*, 951–966, 1989.

Le Méhauté, B., and J. D. Wang, Wave spectrum changes on sloped beach, *J. Waterw. Port Coastal Ocean Div. Am. Soc. Civ. Eng.*, *108*, 33–47, 1982.

Liu, P. L.-F., S. B. Yoon, and J. T. Kirby, Nonlinear refraction-diffraction of waves in shallow water, *J. Fluid Mech.*, *153*, 185–201, 1985.

Mei, C. C., and U. Ünlüata, Harmonic generation in shallow water waves, in *Waves on Beaches*, edited by R. E. Meyer, pp. 181–202, Academic, San Diego, Calif., 1972.

Newell, A. C., and P. J. Aucoin, Semidispersive wave systems, *J. Fluid Mech.*, *49*, 593–609, 1971.

Pawka, S. S., Island shadows in wave directional spectra, *J. Geophys. Res.*, *88*, 2579–2591, 1983.

Peregrine, D. H., Long waves on a beach, *J. Fluid Mech.*, *27*, 815–827, 1967.

Peregrine, D. H., Equations for water waves and the approximations behind them, in *Waves on Beaches and Resulting Sediment Transport*, edited by R. E. Meyer, pp. 95–122, Academic, San Diego, Calif., 1972.

Phillips, O. M., On the dynamics of unsteady gravity waves of finite amplitude, 1, *J. Fluid Mech.*, *9*, 193–217, 1960.

Vincent, C. L., and M. J. Briggs, Refraction-diffraction of irregular waves over a mound, *J. Waterw. Port Coastal Ocean Div. Am. Soc. Civ. Eng.*, *115*, 269–284, 1989.

S. Elgar, School of Electrical Engineering and Computer Science, Washington State University, Pullman, WA 99164-2752.

M. H. Freilich, College of Oceanography, Oregon State University, Corvallis, OR 97331.

R. T. Guza, Center for Coastal Studies 0209, Scripps Institution of Oceanography, La Jolla, CA 92093.

(Received February 8, 1993;
revised July 7, 1993;
accepted July 15, 1993.)